International Journal of Heat and Mass Transfer 123 (2018) 1204–1211

Contents lists available at ScienceDirect

International Journal of Heat and Mass Transfer

journal homepage: www.elsevier.com/locate/ijhmt

# Effective thermal conductivity of packed bed adsorbers: Part 1 – Experimental study

Mina Rouhani, Wendell Huttema, Majid Bahrami *

*Laboratory for Alternative Energy Conversion (LAEC), School of Mechatronic Systems Engineering, Simon Fraser University, BC V3T0A3, Canada*

ARTICLE INFO

*Article history:*
Received 5 July 2017
Received in revised form 16 December 2017
Accepted 31 January 2018
Available online 15 February 2018

*Keywords:*
Effective thermal conductivity
Thermal contact resistance
Packed bed adsorber
AQSOA FAM-Z02
Adsorption thermal energy storage
Heat flow meter

ABSTRACT

Low thermal conductivity in packed bed adsorbers is a crucial challenge facing widespread adoption of low-grade heat adsorption thermal energy storage systems. In this work, thermal conductivities of 2-mm diameter AQSOA FAM-Z02 packed bed adsorbers with different numbers of adsorbent layers are measured, using a NETZSCH HFM 436/3/1E Lambda, in the temperature range of 10–80 °C and under atmospheric pressure. Effects of thermal contact resistance (TCR) between the adsorbent particles and the bed metal surfaces are deconvoluted from the total thermal resistance. Effective thermal conductivities of the adsorber packed bed are 0.188 and 0.204 $W\,m^{-1}\,K^{-1}$ at temperatures of 10 and 80 °C, respectively. It is observed that the relative importance of TCR compared to the total thermal resistance of a monolayer FAM-Z02 packed bed, is 67% at 25 °C and under contact pressure of 0.7 kPa, which is significant and should be considered in the design of adsorption systems.



## 1. Introduction

Concerns over increase in global primary energy consumption [1], greenhouse gas emissions, climate change [2], enormous amount of wasted energy [3], and dependency on the conventional fossil fuel energy resources [4] have made researchers eager for seeking low-grade heat driven sustainable heating and cooling methods. Adsorption technologies, including adsorption thermal energy storage (ATES) [5], adsorption cooling systems [6], adsorption heat pumps [7], and desiccant air conditioning systems [8], can steer the energy sources toward low-carbon sustainable alternatives, e.g., thermal solar, industrial low-grade waste-heat and geothermal energy. ATES can contribute to a significant reduction in the global energy consumption by storing energy of heat sources with intermittent nature, such as solar energy or waste heat, offering high energy storage density and low heat loss. Using non-toxic and non-polluting refrigerants are other environmental benefits that increase attractiveness of ATES. However, the low thermal conductivity of adsorbent materials (0.1–0.8 $W\,m^{-1}\,K^{-1}$ [9]) and high thermal contact resistance between adsorbent and adsorber bed heat exchanger surfaces, hereinafter called TCR, suppress the overall performance and reduce the competitiveness of the available ATES systems.

To tackle the low heat transfer inside the adsorber beds, using composite adsorbents with high thermal conductive additives was found a practical solution [10]. To this end, granular activated carbon with aluminum additives [11], activated carbon with $CaCl_2$ [12], consolidated NaX Zeolite with expanded natural graphite [13], and silica gel-expanded graphite [14] were studied. Consolidated composite adsorbents increase the heat transfer rate in the adsorber beds, however, they may decrease the mass transfer rate [10]. In contrast, a thin layer (less than 1 mm) of coated adsorbent on the metal surface of an adsorber bed: (i) increases the mass transfer between the adsorbate and coated adsorbent, (ii) reduces the pressure drop inside the bed, and (iii) provides a higher heat transfer rate by reducing the TCR between the adsorbent and metal surface of adsorber bed [15].

Consolidated high conductive composites and coated adsorbent increase the heat transfer, whereas granular packed beds provide higher performance in terms of volumetric cooling power (i.e. cooling power divided by volume) and energy storage density (i.e. stored energy divided by volume) for adsorption systems [16]. Freni et al. [16] compared identical heat exchangers, one with 0.1 mm thickness coated adsorbent and the other one with 0.6–0.7 mm diameter loose grain AQSOA FAM-Z02 and showed that even though coated bed provided faster water uptake rate, the granular adsorber offered higher volumetric cooling power.

To study the heat transfer performance of a packed bed adsorber, TCR and effective thermal conductivity of the packed bed should be measured and modeled properly. Importance of TCR

* Corresponding author.
*E-mail addresses:* mrouhani@sfu.ca (M. Rouhani), wah@sfu.ca (W. Huttema), mbahrami@sfu.ca (M. Bahrami).

https://doi.org/10.1016/j.ijheatmasstransfer.2018.01.142
0017-9310/

**Nomenclature**

| | |
|---|---|
| $A$ | surface area of the packed bed, $cm^2$ |
| ATES | adsorption thermal energy storage |
| $d_p$ | adsorbent particle diameter, mm |
| $f_{calib}$ | calibration factor of the heat flux transducer, $W\,m^{-2}\,V^{-1}$ |
| HFM | heat flowmeter |
| $k$ | thermal conductivity, $W\,m^{-1}\,K^{-1}$ |
| $k_{tot}$ | packed bed total thermal conductivity (effects of TCR is included.), $W\,m^{-1}\,K^{-1}$ |
| $k_{eff,bed}$ | packed bed effective (medium) thermal conductivity (effects of TCR is not included.), $W\,m^{-1}\,K^{-1}$ |
| $L$ | packed bed length (thickness), mm |
| $\omega$ | water uptake, $kg\,kg_{ads}^{-1}$ |
| $n$ | number of adsorbent layers |
| $P$ | gas pressure, Pa |
| $P_{contact}$ | contact pressure at the contact of adsorbent particle and the metal surface, Pa |
| $\dot{Q}$ | heat flow, W |
| $R$ | thermal resistance, $K\,W^{-1}$ |
| $R_{as-p}$ | thermal contact resistance between the aluminum sheet and the particles, $K\,W^{-1}$ |
| $R_{bed}$ | packed bed effective thermal resistance (excluding the TCR), $K\,W^{-1}$ |
| $R_p$ | thermal resistance of adsorbent particle, $K\,W^{-1}$ |
| $R_{p-p}$ | thermal contact resistance between the particles, $K\,W^{-1}$ |
| $R_{tot}$ | packed bed total thermal resistance (including the TCR), $K\,W^{-1}$ |
| $t$ | time, s |
| $T$ | temperature, K |
| $T_1$ | temperature of the upper hot plate of the heat flowmeter, K |
| $T_2$ | temperature of the lower cold plate of the heat flowmeter, K |
| $TCR$ | thermal contact resistance, $K\,W^{-1}$ |
| $V$ | heat flux transducer output, V |

*Subscripts*

| | |
|---|---|
| *as* | aluminum sheet |
| *bed* | packed bed |
| *contact* | at the contact of adsorbent particles and the heat exchanger metal surface |
| *eff* | effective |
| *p* | adsorbent particle |
| *tot* | total |
| *w* | water |

has been raised in the literature [17–19], but little has been shown regarding the measurement and modeling of TCR inside the adsorber bed. Based on the test procedure for flat surfaces developed by Antonetti and Yovanovich [20], Wang et al. [21] measured the TCR between the heat exchanger surface and zeolite granule adsorbent with diameters of 0.297, 0.149 and 0.074 mm by heat flux ratio-measuring instrument, under vacuum pressure. A correlation fitted to their experimental data [21] was fed into an empirical lumped analytical model for thermal conductivity of a silica gel packed bed, developed by Rezk et al. [22]. Sharafian et al. [19] experimentally showed that the ratio of TCR to the total thermal resistance could be as high as 26% at 37 °C, for a consolidated block of silica gel-PVP on a metal substrate.

Thermal conductivity measurement methods used for various adsorbent materials are listed in Table 1. Bjurström et al. [23] measured thermal conductivity of moist silica gel particles by transient hot strips method and effective thermal conductivity of a dry packed bed of silica gel through a steady-state measurement, using a custom-built annular test bed. Tanashev and Aristov [24] measured thermal conductivity of a composite of KSK silica gel and $CaCl_2$ by the transient hot wire method at 290–330 K and atmospheric pressure. They showed that thermal conductivity of the composite increased from 0.112 to 0.216 $W\,m^{-1}\,K^{-1}$ when water uptake was raised from 0.01 to 0.58 $kg\,kg_{ads}^{-1}$. Tanashev et al. [25] later showed that their reported thermal conductivity of the composites of silica gel and salts, under atmospheric pressure, could be used in the closed adsorption systems as well, since their results showed that thermal conductivity was a stronger function of uptake rather than vapor pressure and temperature.

Due to the adsorption heat released by adsorbents, the measured temperature difference in the unsteady thermal conductivity measurement is smaller than that of the test with no adsorption

**Table 1**
Thermal conductivity measurement techniques used for adsorbent materials in the literature.

| Ref. | Measurement method | Standard | Adsorbent | Adsorbent configuration | Uptake, $kg\,kg_{ads}^{-1}$ | Temperature, K | Thermal conductivity, $W\,m^{-1}\,K^{-1}$ | Importance of TCR (TCR $R_{tot}^{-1}$) |
|---|---|---|---|---|---|---|---|---|
| [23] | Transient hot strip/ transient plane source | ISO22007-2 | Silica gel | Packed bed (silica gels are poured in a cell (40 × 60 × 10 mm) | 0 | 295 | 0.147 | – |
| | | | | | 0.329 | 295 | 0.265 | – |
| [26] | | | Silica gel + $CaCl_2$ + 20 wt% graphite flakes | Composite | 0.18 | 308 | 0.41 | – |
| [24] | Transient hot wire | ASTM C1113 | Silica gel KSK + 20 wt% $CaCl_2$ | Composite | 0.01 | 293 | 0.112 ± 0.007 | – |
| | | | | | 0.58 | 293 | 0.216 ± 0.012 | – |
| [27] | | | Silica gel + 36.6 wt% $CaCl_2$+ binder $Al(OH)_3$ | Composite | 0.053 | 363 | 0.12 | – |
| | | | | | 0.286 | 363 | 0.227 | – |
| [28] | | | AQSOA FAM-Z02 | – | – | 303 | 0.117 | – |
| | | | | | – | 363 | 0.128 | – |
| [29] | Laser flash | ASTM E1461-13 | AQSOA FAM-Z01 | Coated (0.3 mm thickness) | – | 293 | 0.376 | – |
| [30] | Guarded-hot plate | BS-874 | Monolithic carbon (sample LM127) | Monolithic with coarse powders | – | 293 | 0.45 | – |
| | | | | | – | 393 | 0.4 | – |
| [19] | | ASTM E1530 | Silica gel + PVP with a metallic substrate | Composite | – | 310 | 0.282 | 0.26 |
| | | | | | – | 321 | 0.240 | 0.05 |

heat, which results in higher thermal conductivity [31]. To eliminate the above-mentioned error in the thermal conductivity measurement of adsorbent materials, steady-state measurements have been found more practical [31]. Sharafian et al. [19] conducted a steady state measurement with a custom-built guarded-hot plate device to measure the thermal conductivity of consolidated silica gel-PVP samples with volume of $25.4 \times 25.4 \times 6.6\ mm^3$.

Effective heat and mass transfer properties of an adsorber bed are strongly dependent on the size of the adsorber bed [9]. Water uptake rate and thermal conductivity measurements of small amount of adsorbent material, less than 0.1 kg, can only show an ideal design and, instead, a large-scale measurement is essential to realistically study the heat and mass transfer in a packed bed adsorber. Table 2 shows the difference between thermal conductivity of solid grain and packed bed of adsorbent materials, reported in the Ref. [9]. Hence, in this work, a steady-state heat flow meter with a test chamber volume of $305 \times 305 \times 100\ mm^3$ was selected to measure thermal conductivity of a large-scale packed bed.

AQSOA FAM-Z02, hereinafter called FAM-Z02, is a synthetic zeolite-based adsorbent material with high durability (reported 60,000 cycles) and high adsorption capacity (6-fold higher than that of A-type silica gel), developed by Mitsubishi Chemical Ltd [32,28]. Coated and loose grain FAM-Z02 were recently utilized in adsorption systems and showed promising performance [16,33–37]. Showing successful operation, it is desirable to carry out precise measurement of thermal conductivity of FAM-Z02, at different temperature and water uptake, to better analyze and optimize adsorption systems using FAM-Z02/water as the working pair.

Little information is available concerning thermal properties of FAM-Z02, listed in Table 3. Okamoto et al. [29] used transient hot wire method to measure thermal conductivity of FAM-Z02 powder. They reported thermal conductivity of 0.117 and 0.128 $W\ m^{-1}\ K^{-1}$ at 303 and 363 K, respectively. Effective thermal conductivity of coated FAM-Z02 with a clay as the binder was studied by Frazzica et al. [38]. They reported effective thermal conductivity of 0.28 $W\ m^{-1}\ K^{-1}$ for 0.6 mm coated FAM-Z02 [38] .

Girnik and Aristov [34] studied the kinetics of different number of layers (n = 2, 4, and 8) of FAM-Z02 grains, using large temperature jump method, which was developed by Aristov et al. [40]. To the authors' knowledge, there is no experimental data regarding thermal conductivity of a packed bed of FAM-Z02 at various temperatures, uptake, contact pressure and number of layers, available in the literature.

This study aims to provide the first set of experimental data on the effective thermal conductivity of 2-mm diameter FAM-Z02 packed beds, for different numbers of adsorbent layers, temperatures, and contact pressures. To measure thermal conductivity of a loose grain packed bed adsorber, heat flow meter method is applied as a reliable steady state measurement method for low conductive materials. The TCR between the adsorbent particles and the heat exchange media is deconvoluted from the total bed resistance to study the relative importance of TCR in packed beds.

**Table 2**
Comparison between thermal conductivity of a solid grain adsorbent and a packed bed adsorber reported in the literature [9].

| Adsorbent material | Adsorbent configuration | Thermal conductivity, $W\ m^{-1}\ K^{-1}$ |
|---|---|---|
| Zeolite | Solid grain | 0.18–0.4 |
| | Granular bed ($H_2O$) | 0.03–0.15 |
| Silica gel | Solid grain | 0.37–0.8 |
| | Granular bed | 0.05–0.2 |
| | Granular bed ($H_2O$) | 0.04–0.26 |
| Activated carbon | Solid grain | 0.54 |
| | Granular bed | 0.3–0.5 |
| | Granular bed (methanol) | 0.14–0.17 |

## 2. Experimental study

In this study, a heat flow meter apparatus (HFM 436/3/1E Lambda, NETZSCH Instruments) was used for steady-state thermal conductivity measurements of packed bed adsorbers. The HFM can measure samples with thermal conductivities of 0.002 to 2.0 $W\ m^{-1}\ K^{-1}$, with an accuracy of ±1–3%. The HFM, shown in Fig. 1a, can apply a variable external load on the sample (see Fig. 1b), to control the contact pressure and ensure a uniform contact between the upper and lower plates and the sample, throughout the plate surface. Heat-flow transducers (flux gages) are installed in the center of the test chamber and far from the frame. Measurements were carried out at mean temperatures from 10 to 80 °C and 20 K temperature difference between the hot (upper) and cold (lower) plates.

Packed beds of 2 mm diameter FAM-Z02 spherical particles were prepared with 1, 2, 4 and 6 layers. Similar to a real finned adsorber bed, the adsorbent particles were randomly packed, and as shown in Fig. 1c and d, adsorbent layers were sandwiched between two aluminum sheets ($305 \times 305 \times 0.4\ mm^3$). Narrow adhesive-back EPDM foam strips (Neoprene/EPDM/SBR foam with closed cell), which restricted water and air from being exchanged between the packed bed and the environment [41], were attached around the perimeter of the lower aluminum sheet, forming a frame to hold the adsorbent particles (see Fig. 1c and e). Measurements were carried out after the adsorbents reached the equilibrium at the room condition (24 °C and 35% RH). Afterwards, the custom-built sample holder was covered with the upper aluminum sheet and was placed in the test chamber, where it was pressed between the hot and cold plates under the preset contact pressure. Since there was no air exchange between the packed bed and the test chamber environment, if all the water that was in the air inside the packed bed had been adsorbed, the adsorbent water content would have changed only by $1.5 \times 10^{-5}\ kg\ kg_{ads}^{-1}$. At 80 °C, the air could hold an additional $0.28\ kg\ m_{air}^{-3}$ of water vapor. If this all had came from the adsorbent, the water content would have decreased by $5.3 \times 10^{-4}\ kg\ kg_{ads}^{-1}$. Thus, the adsorbent water uptake showed negligible change. As shown in Fig. 1d and e, two auxiliary K-type thermocouples were attached to the aluminum sheets, adjacent to the adsorbent medium, to eliminate the effects of the thermal resistance of the aluminum sheets as well as the TCR between the hot/cold plates and aluminum sheets.

The HFM was configured to heat the samples from the top to avoid the natural convection [42,43]. Moreover, natural convection in the packed beds with small voids is negligible [44]. The measured thermal resistance was the total thermal resistance between the isothermal surfaces at temperatures of $T_1$ and $T_2$ (see Fig. 2a). The associated thermal resistance network of the 4-layer packed bed adsorber is illustrated in Fig. 2b and the total thermal resistance of n-layer packed bed adsorber is as follows:

$$R_{tot} = L_{bed}/(k_{tot}A) = 2R_{as-p} + nR_p + (n-1)R_{p-p} = 2R_{as-p} + R_{bed} = TCR + R_{bed} \quad (1)$$

where $R_{as-p}$ is the thermal contact resistance between the aluminum sheet and the particles and $R_{p-p}$ is the thermal contact resistances between the adsorbent particles. *TCR* accounts for the total thermal contact resistance of upper and lower aluminum sheets and adsorbent particle ($2R_{as-p}$). The maximum measurement

**Table 3**
Properties of SAPO-34 CHA and FAM-Z02 (commercial SAPO-34 CHA).

| Ref. | Adsorbent | Adsorbent configuration | Specific heat capacity, J $kg^{-1}$ $K^{-1}$ | Bulk density, kg $m^{-3}$ | Thermal conductivity, W $m^{-1}$ $K^{-1}$ | Thermal diffusivity, $m^2$ $s^{-1}$ |
|---|---|---|---|---|---|---|
| [29] | FAM-Z02 | Powder | 822 (303 K)<br>942 (363 K) | 600–700 | 0.117 (303 K)<br>0.128 (343 K) | $2.19 \times 10^{-7}$<br>$2.09 \times 10^{-7}$ |
| [38] | FAM-Z02 + 18.5 wt% Bentonite clay + 1.5 wt% micro carbon fiber | Coated (0.4 mm)<br>Coated (0.6 mm) | 900 | – | 0.44<br>0.28 | – |
| [39] | SAPO-34 CHA + Al | Composite | 900 | 1510 | 9 ± 1 | $6.62 \times 10^{-6}$ |

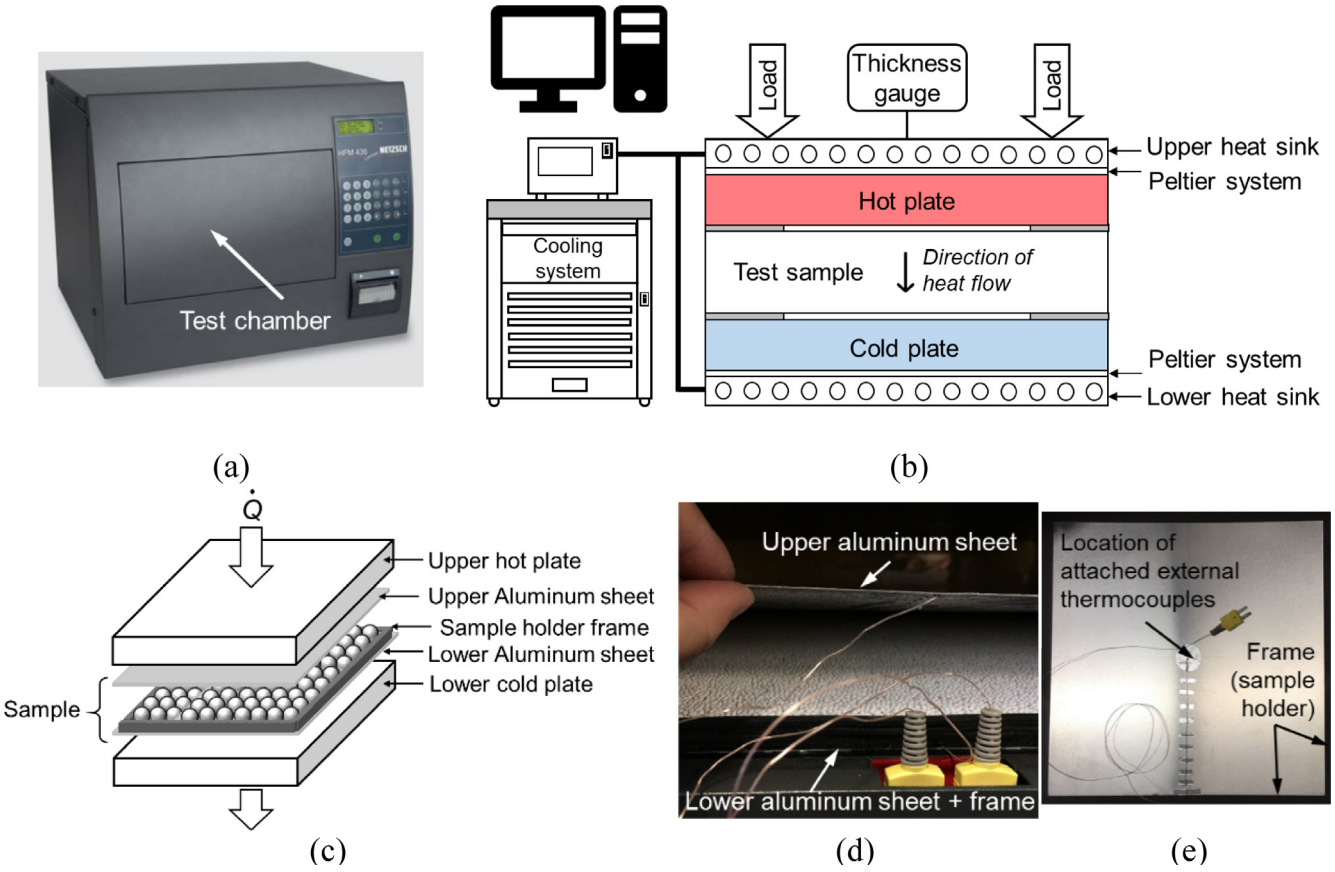


**Fig. 1.** (a) View of instrument and (b) schematic of the NETZSCH HFM 436/3/1 Lambda, (c) schematic of the adsorbent particles inside the HFM test chamber, (d) arrangement of adsorbents between two aluminum sheets, and (e) attached K-type thermocouples to the inner surface of the lower aluminum sheet, and the frame made of EPDM adhesive-back foam strips, used as the sample holder.

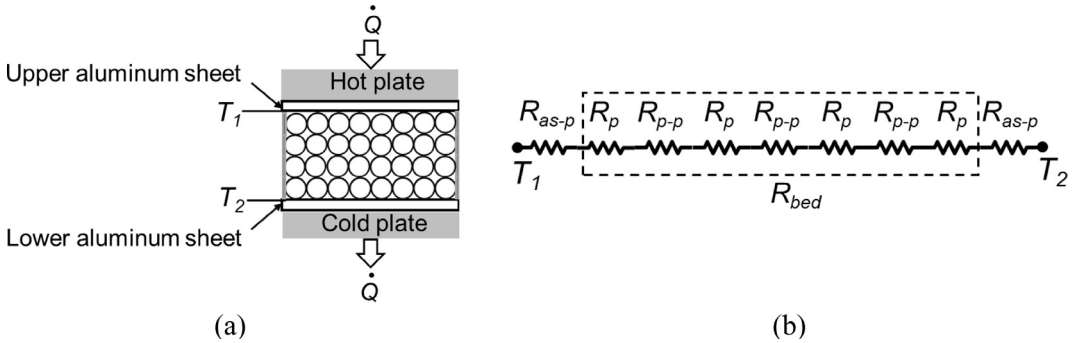


**Fig. 2.** (a) 4-layer packed bed sandwiched between two aluminum sheets and hot and cold plates and (b) equivalent thermal resistance network of the 4-layer packed bed between the attached thermocouples, at temperatures of $T_1$ and $T_2$.

uncertainties of thermal conductivity and thermal resistance are 7–8% and 7% respectively (see Appendix A).

Design and optimization of a packed bed adsorber require the knowledge of the effective thermal conductivity of the adsorbent packed bed medium, which is $k_{eff,bed} = L_{bed}/(AR_{bed})$. The bulk thermal resistance of the packed bed medium, $R_{bed}$, includes the bulk thermal resistance of the adsorbent particle, $R_p$, and the contact resistance between the particles, $R_{p-p}$. Thus, the measured effective thermal conductivity of the packed bed, $k_{eff,bed}$, is independent of the properties of the heat exchanger surface and can be used for 2-mm FAM-Z02 randomly packed beds in different heat exchanger designs, but under the same operating conditions. To this end, TCR should be deconvoluted from the measured total resistance , $R_{tot}$. By measuring the total thermal resistances for (at least) two different numbers of adsorbent layers (i.e. different bed thicknesses), it is possible to deconvolute the *TCR* from the total resistance. In this method, at each mean temperature, an identical *TCR* is assumed for different bed thicknesses, due to the similarities in microstructure and bed arrangement. Therefore, the *TCR* and effective thermal conductivity of packed bed medium are calculated from Eq. (2), for two-thickness method or multiple-thickness method [45], and the slope and intercept of the line fitted to the $R_{tot}$ versus the bed thickness are $1/(k_{eff,bed}A)$ and *TCR*, respectively.

$$R_{tot,1} = TCR + \frac{L_1}{k_{eff,bed}A}$$
$$R_{tot,2} = TCR + \frac{L_2}{k_{eff,bed}A} \quad (2)$$
$$k_{eff,bed} = \frac{(L_2 - L_1)}{A(R_{tot,2} - R_{tot,1})}$$

## 3. Results and discussion

$R_{tot} \cdot A$ versus the bed thickness (or number of the adsorbent layers) for 2-mm FAM-Z02 packed bed adsorber at three temperatures of 25, 60 and 80 °C is plotted in Fig. 3. $R_{tot} \cdot A$ decreases with the temperature of the bed, since the adsorbent thermal conductivity and packed bed total thermal conductivity increase with a rise in the mean temperature. As illustrated in Fig. 3, $R_{tot} \cdot A$ increases with an increase in the number of layers (bed thickness). To find the packed bed effective thermal conductivity, the effects of *TCR* should be deconvoluted from the packed bed total thermal resistance, as discussed in Section 2. Hence, $k_{eff,bed}$ and *TCR* are extracted from the slope and intercept of the linear fit to Fig. 3.

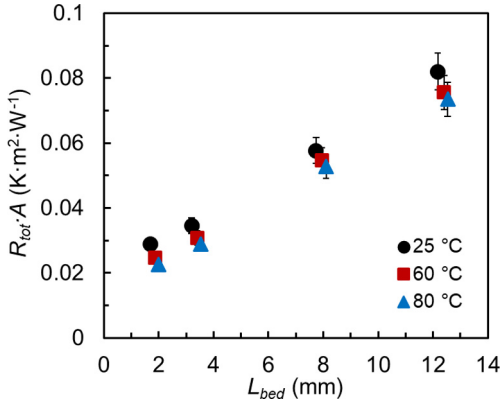


**Fig. 3.** $R_{tot} \cdot A$ versus bed thickness of 2-mm FAM-Z02 packed beds for 1, 2, 4, and 6 layers, with water uptake of 0.30 ± 0.02 kg $kg_{ads}^{-1}$, at temperatures of 25, 60 and 80 °C under contact pressures of 0.7 kPa.

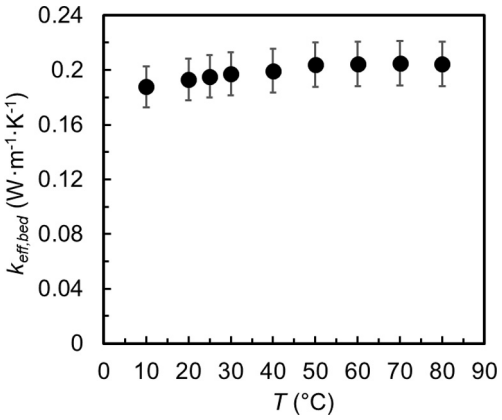


**Fig. 4.** Packed bed effective thermal conductivity versus the mean temperature, with water uptake of 0.30 ± 0.02 kg $kg_{ads}^{-1}$ and under contact pressure of 0.7 kPa.

Changes in $k_{eff,bed}$ versus the bed mean temperature is plotted in Fig. 4, in which the effects of the *TCR* is deconvoluted. Effective thermal conductivity of the 2-mm diameter FAM-Z02 randomly-packed bed adsorber varies between 0.1878 and 0.2043 $W\,m^{-1}\,K^{-1}$, and slightly increases with an increase in temperature. Since the measurements were performed at atmospheric pressure, the measured thermal conductivity can be used for open adsorption systems, including open ATES and desiccant air conditioning and dehumidification systems. For closed adsorption systems, these measured thermal conductivity values may lead to an overestimation of performance.

The relative importance of *TCR* to the total thermal resistance of a 2-mm FAM-Z02 packed bed is shown in Fig. 5, for temperatures varying between 10 and 80 °C and number of layers of 1, 2, 4, and 6. The contact pressure on the hot and cold plates, $P_{contact}$, is 0.7 kPa. At 25 °C and atmospheric pressure, *TCR* forms 67% of the total thermal resistance of a monolayer of FAM-Z02, which clearly shows the significant importance of *TCR* in the packed bed adsorbers. As expected, *TCR* becomes more important for lower number of layers of adsorbent and at lower temperatures. Since higher uptake rate and higher specific cooling power are achieved for the monolayer of adsorbent materials, *TCR* is a serious issue which should be taken into consideration. *TCR* decreases 54%, when temperature increases from 25 to 80 °C. This is due, in part, to the higher thermal conductivity of air at higher temperatures. Since porosity in a packed bed of spheres is larger near its boundaries [46,47], and the filling gas (air) has higher share of contact area with the

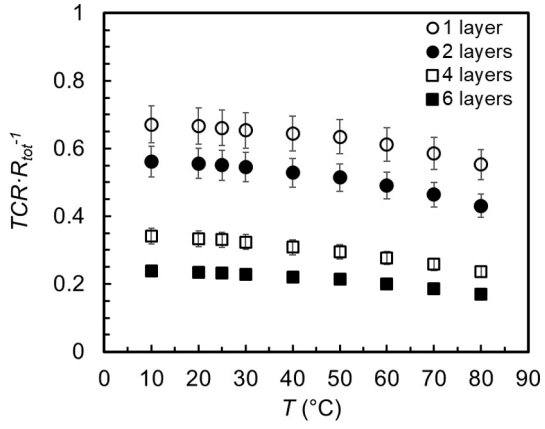


**Fig. 5.** Measured values for relative importance of TCR to the total thermal resistance at temperatures of 10 to 80 °C, contact pressure of 0.7 kPa and for 1, 2, 4, and 6 layers of FAM-Z02 with water uptake of 0.30 ± 0.02 kg $kg_{ads}^{-1}$.

aluminum sheets, the increase in the air thermal conductivity has more effect on the thermal contact conductance ($1/TCR$), compared to the effective thermal conductivity of packed bed medium. The other sources of this increase in $TCR$ are unclear, but it could be due to the changes in packed bed configuration and contact points at higher temperatures.

The measured values of $TCR \cdot A$ for two contact pressures of 0.7 and 1.4 kPa are plotted in Fig. 6. By increasing the contact pressure (compression), $TCR \cdot A$ decreases due to a better contact between adsorbent and the heat exchanger surface. This reduction in $TCR \cdot A$, due to the higher contact pressure, is faded away by increasing the temperature; $TCR \cdot A$ increases by 6% and less than 1.5% at 10 and 80 °C, respectively, when the contact pressure increases by 0.7 kPa from 0.7 to 1.4 kPa.

Additionally, effect of temperature cycling on the total thermal conductivity, $k_{tot}$ (see Eq. (1)), was investigated for a 6-layer FAM-Z02 packed bed adsorber. As shown in Fig. 7a, the packed bed adsorber was subjected to 4 cycles between 25 and 80 °C. During the temperature cycles, subtle changes in $k_{tot}$ are discerned (Fig. 7b), i.e., maximum relative difference in $k_{tot}$ is 1% for both temperatures. This indicates the good repeatability of the measurements and negligible hysteresis effects in the water uptake and thermal conductivity of FAM-Z02, as expected and widely reported in the literature [28], [48]. The measured $k_{tot}$ is 0.143 W m$^{-1}$ K$^{-1}$ (compared to $k_{eff,bed}$ of 0.195 W m$^{-1}$ K$^{-1}$) at 25 °C and 0.164 W m$^{-1}$ K$^{-1}$ (compared to $k_{eff,bed}$ of 0.204 W m$^{-1}$ K$^{-1}$) at 80 °C; the difference between the total thermal conductivity and the effective thermal conductivity is due to the TCR.

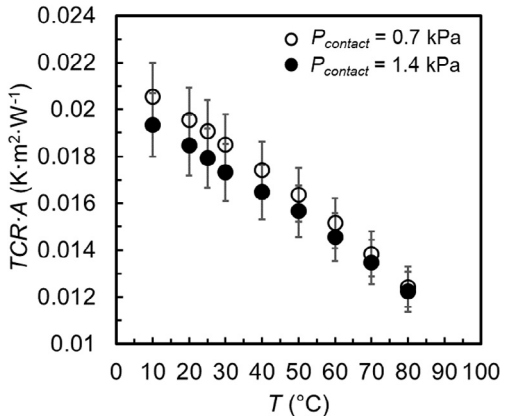


**Fig. 6.** Effect of contact pressure on the measured $TCR \cdot A$ for 2-mm FAM-Z02 packed bed with water uptake of 0.30 ± 0.02 kg $kg_{ads}^{-1}$.

## 4. Conclusions

In this study, total thermal conductivity of a 2 mm-diameter FAM-Z02 packed adsorber bed was measured by HFM, at temperatures of 10 to 80 °C and number of adsorbent layers of 1, 2, 4 and 6 and under contact pressures of 0.7 and 1.4 kPa. Effects of $TCR$ were deconvoluted from the total thermal resistance of the packed bed adsorber and the relative importance of $TCR$ to the total thermal resistance was demonstrated. $TCR/R_{tot}$ of a monolayer 2-mm FAM-Z02 packed bed, was 67% at 25 °C. Effective thermal conductivity of the FAM-Z02 randomly packed bed was 0.188–0.204 W m$^{-1}$ K$^{-1}$ for temperatures between 10 and 80 °C. Increasing the compression pressure from 0.7 to 1.4 kPa decreased the $TCR \cdot A$ by 6% for mean temperature of 10 °C and 1.5% for mean temperature of 80 °C. Absence of hysteresis effect and repeatability of the thermal conductivity measurement of the FAM-Z02 loose grain packed bed were proved for 4 heating–cooling cycles between temperatures of 25 and 80 °C.

## Acknowledgements

The authors gratefully acknowledge the financial support of the Natural Sciences and Engineering Research Council of Canada (NSERC) through the Automotive Partnership Canada Grant No. APCPJ 401826-10. We thank Drs. Claire McCague from LAEC, and Marc-Antoine Thermitus from NETZSCH Instruments, North America, for valuable discussion.

## Appendix A. Measurement uncertainty

The operational definition of thermal conductivity, for HFM measurement, is obtained from the following equation (ASTM C 518),

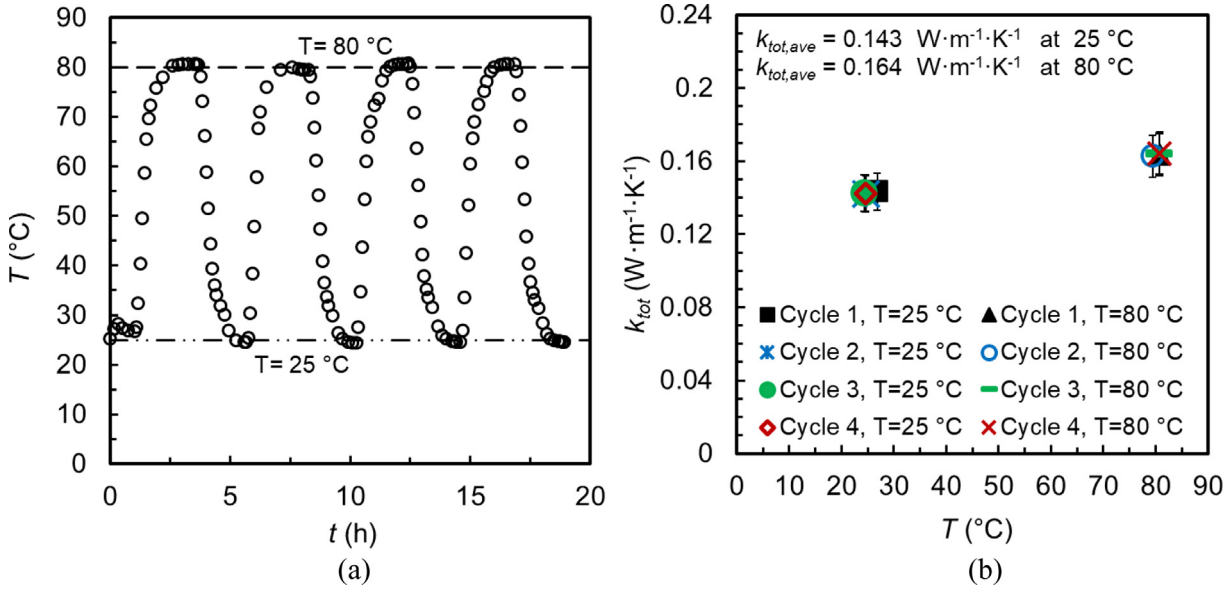


**Fig. 7.** (a) Cyclic temperature changes between 25 °C and 80 °C, and (b) effects of cyclic temperature change on the total thermal conductivity of 6-layer 2 mm FAM-Z02 packed beds with water uptake of 0.30 ± 0.02 kg $kg_{ads}^{-1}$ and under 0.7 kPa contact pressure.

**Table A1**
Accuracies and relative error of HFM measurements.

| $\delta L_{bed}$(cm) | $\delta T$(°C) | $\delta V$(μV) | $\left(\frac{\delta f_{calib}}{f_{calib}}\right)$ | $\left(\frac{\delta L_{bed}}{L_{bed}}\right)$ | $\left(\frac{\delta V}{V}\right)$ | $\frac{\delta(\Delta T)}{\Delta T}$ |
|---|---|---|---|---|---|---|
| 0.01 | 1 (external thermocouple) | 5 | 0.01 | 0.008–0.036 | $2 \times 10^{-4}$ | 0.05 |

$$k = \frac{f_{calib} V L_{bed}}{\Delta T} \tag{A1}$$

where $f_{calib}$[W/(m$^2$V)] is the calibration factor, and $V$[V] is the heat flux transducer output. Therefore, According to the uncertainty propagation [49], the systematic error of the thermal conductivity is as follows,

$$\frac{\delta k}{k} = \left[\left(\frac{\delta f_{calib}}{f_{calib}}\right)^2 + \left(\frac{\delta V}{V}\right)^2 + \left(\frac{\delta L_{bed}}{L_{bed}}\right)^2 + \left(\frac{\delta(\Delta T)}{\Delta T}\right)^2\right]^{1/2} \tag{A2}$$

where the last term in the right-hand side of this equation is calculated as follows,

$$\frac{\delta(\Delta T)}{\Delta T} = \left[\left(\frac{\delta T_1}{\Delta T}\right)^2 + \left(\frac{\delta T_2}{\Delta T}\right)^2\right]^{1/2} \tag{A3}$$

The accuracies and relative errors of bed thickness, heat flux measurement and calibration factor (supplied by the manufacturer) and external thermocouples are listed in Table A1. The systematic uncertainty of thermal conductivity is 7–8%. The difference between the thermal conductivity uncertainty of the experiment and the reported value by manufacturer is due to the thermocouple accuracy of the external thermocouples (±1 °C) compared to that of the embedded thermocouples in HFM (±0.01 °C). As mentioned before, external thermocouples are used to eliminate the effect of thermal contact resistance between the hot/cold plate and the sample.

Similarly, uncertainty of thermal resistance is calculated as follows,

$$\frac{\delta R}{R} = \left[\left(\frac{\delta f_{calib}}{f_{calib}}\right)^2 + \left(\frac{\delta V}{V}\right)^2 + \left(\frac{\delta(\Delta T)}{\Delta T}\right)^2\right]^{1/2} \tag{A4}$$

Therefore, the maximum systematic uncertainty of thermal resistance is 7%. The random error from the repeatability measurement is negligible.

## References


[1] International Energy Agency, Key World Energy Statistics, 2016.
[2] S. Anand, A. Gupta, S.K. Tyagi, Solar cooling systems for climate change mitigation: a review, Renew. Sustain. Energy Rev. 41 (2015) 143–161.
[3] U.S. DOE, Quadrennial Technology Review: An Assessment of Energy Technologies and Research Opportunities.
[4] K.F. Fong, T.T. Chow, C.K. Lee, Z. Lin, L.S. Chan, Comparative study of different solar cooling systems for buildings in subtropical city, Sol. Energy 84 (2) (2010) 227–244.
[5] A. Hauer, Thermal Energy Storage with Zeolite for Heating and Cooling Applications, in: International Sorption Heat Pump Conference 2002, 2002, pp. 385–390.
[6] I.S. Girnik, Y.I. Aristov, Making adsorptive chillers more fast and efficient: the effect of bi-dispersed adsorbent bed, Appl. Therm. Eng. 106 (2016) 254–256.
[7] B.N. Okunev, A.P. Gromov, L.I. Heifets, Y.I. Aristov, A new methodology of studying the dynamics of water sorption/desorption under real operating conditions of adsorption heat pumps: modelling of coupled heat and mass transfer in a single adsorbent grain, Int. J. Heat Mass Transf. 51 (1–2) (2008) 246–252.
[8] A.A. Pesaran, A.F. Mills, Moisture transport in silica gel packed beds—II. Experimental study, Int. J. Heat Mass Transf. 30 (6) (1987) 1051–1060.
[9] K.E. N'Tsoukpoe, G. Restuccia, T. Schmidt, X. Py, The size of sorbents in low pressure sorption or thermochemical energy storage processes, Energy 77 (2014) 983–998.
[10] S.G. Wang, R.Z. Wang, X.R. Li, Research and development of consolidated adsorbent for adsorption systems, Renew. Energy 30 (9) (2005) 1425–1441.
[11] A.A. Askalany, S.K. Henninger, M. Ghazy, B.B. Saha, Effect of improving thermal conductivity of the adsorbent on performance of adsorption cooling system, Appl. Therm. Eng. 110 (2017) 695–702.
[12] L.W. Wang, R.Z. Wang, Z.S. Lu, C.J. Chen, K. Wang, J.Y. Wu, The performance of two adsorption ice making test units using activated carbon and a carbon composite as adsorbents, Carbon N. Y. 44 (13) (2006) 2671–2680.
[13] F. Poyelle, J. Guilleminot, F. Meunier, Experimental tests and predictive model of an adsorptive air conditioning unit, Ind. Eng. Chem. Res. 38 (1) (1999) 298–309.
[14] T.H. Eun, H.K. Song, J. Hun Han, K.H. Lee, J.N. Kim, Enhancement of heat and mass transfer in silica-expanded graphite composite blocks for adsorption heat pumps: Part I. Characterization of the composite blocks, Int. J. Refrig. 23 (1) (2000) 64–73.
[15] A. Freni, B. Dawoud, L. Bonaccorsi, S. Chmielewski, A. Frazzica, L. Calabrese, G. Restuccia, Characterization of Zeolite-Based Coatings for Adsorption Heat Pumps, Cham, Springer briefs in applied sciences and technology: Springer, 2015.
[16] A. Freni, L. Bonaccorsi, L. Calabrese, A. Caprì, A. Frazzica, A. Sapienza, SAPO-34 coated adsorbent heat exchanger for adsorption chillers, Appl. Therm. Eng. 82 (2015) 1–7.
[17] A. Rezk, R.K. Al-Dadah, S. Mahmoud, A. Elsayed, Effects of contact resistance and metal additives in finned-tube adsorbent beds on the performance of silica gel/water adsorption chiller, Appl. Therm. Eng. 53 (2) (2013) 278–284.
[18] X.H. Li, X.H. Hou, X. Zhang, Z.X. Yuan, A review on development of adsorption cooling - Novel beds and advanced cycles, Energy Convers. Manage. 94 (2015) 221–232.
[19] A. Sharafian, K. Fayazmanesh, C. McCague, M. Bahrami, Thermal conductivity and contact resistance of mesoporous silica gel adsorbents bound with polyvinylpyrrolidone in contact with a metallic substrate for adsorption cooling system applications, Int. J. Heat Mass Transf. 79 (2014) 64–71.
[20] V.W. Antonetti, M.M. Yovanovich, Enhancement of thermal contact conductance by metallic coatings: theory and experiment, J. Heat Transfer 107 (3) (1985) 513–519.
[21] D. Zhu, S. Wang, Experimental investigation of contact resistance in adsorber of solar adsorption refrigeration, Sol. Energy 73 (3) (2002) 177–185.
[22] A.R.M. Rezk, R.K. Al-Dadah, Physical and operating conditions effects on silica gel/water adsorption chiller performance, Appl. Energy 89 (1) (2012) 142–149.
[23] H. Bjurström, E. Karawacki, B. Carlsson, Thermal conductivity of a microporous particulate medium: moist silica gel, Int. J. Heat Mass Transf. 27 (11) (1984) 2025–2036.
[24] Y.Y. Tanashev, Y.I. Aristov, Thermal conductivity of a silica gel + calcium chloride system: the effect of adsorbed water, J. Eng. Phys. Thermophys. 73 (5) (2000) 876–883.
[25] Y.Y. Tanashev, A.V. Krainov, Y.I. Aristov, Thermal conductivity of composite sorbents 'salt in porous matrix' for heat storage and transformation, Appl. Therm. Eng. 61 (2) (2013) 401–407.
[26] K. Fayazmanesh, C. McCague, M. Bahrami, Consolidated adsorbent containing graphite flakes for heat-driven water sorption cooling systems, Appl. Therm. Eng. 123 (2017) 753–760.
[27] A. Freni, M.M. Tokarev, G. Restuccia, A.G. Okunev, Y.I. Aristov, Thermal conductivity of selective water sorbents under the working conditions of a sorption chiller, Appl. Therm. Eng. 22 (14) (2002) 1631–1642.
[28] H. Kakiuchi, M. Iwade, S. Shimooka, K. Ooshima, "Novel zeolite adsorbents and their application for AHP and Desiccant system," IEA-Annex, 2005.
[29] K. Okamoto, M. Teduka, T. Nakano, S. Kubokawa, H. Kakiuchi, The development of AQSOA water vapor adsorbent and AQSOA coated heat exchanger, in: The International Sorption Heat Pump Conference 2011, 2010.
[30] Z. Tamainot-Telto, R.E. Critoph, Monolithic carbon for sorption refrigeration and heat pump applications, Appl. Therm. Eng. 21 (1) (2001) 37–52.
[31] L.W. Wang, Z. Tamainot-Telto, S.J. Metcalf, R.E. Critoph, R.Z. Wang, Anisotropic thermal conductivity and permeability of compacted expanded natural graphite, Appl. Therm. Eng. 30 (13) (2010) 1805–1811.
[32] S. Shimooka, K. Oshima, H. Hidaka, T. Takewaki, H. Kakiuchi, A. Kodama, M. Kubota, H. Matsuda, The evaluation of direct cooling and heating desiccant device coated with FAM, J. Chem. Eng. Japan 40 (13) (2007) 1330–1334.
[33] A. Sharafian, S.M. Nemati Mehr, P.C. Thimmaiah, W. Huttema, M. Bahrami, Effects of adsorbent mass and number of adsorber beds on the performance of a waste heat-driven adsorption cooling system for vehicle air conditioning applications, Energy 112 (2016) 481–493.
[34] I.S. Girnik, Y.I. Aristov, Dynamic optimization of adsorptive chillers: the 'AQSOA$^{TM}$-FAM-Z02 – water' working pair, Energy 106 (2016) 13–22.
[35] G. Gullì, A. Sapienza, A. Caprì, F. Costa, D. La Rosa, V. Palomba, A. Freni, Innovative adsorption chiller for marine applications: design and building, Energy Procedia 82 (2015) 432–438.
[36] A. Sapienza, G. Gullì, L. Calabrese, V. Palomba, A. Frazzica, V. Brancato, D. La, S. Vasta, A. Freni, L. Bonaccorsi, G. Cacciola, An innovative adsorptive chiller prototype based on 3 hybrid coated/granular adsorbers, Appl. Energy 179 (2016) 929–938.
[37] A. Frazzica, A. Freni, Adsorbent working pairs for solar thermal energy storage in buildings, Renew. Energy 110 (2016) 87–94.
[38] A. Frazzica, G. Füldner, A. Sapienza, A. Freni, L. Schnabel, Experimental and theoretical analysis of the kinetic performance of an adsorbent coating composition for use in adsorption chillers and heat pumps, Appl. Therm. Eng. 73 (1) (2014) 1022–1031.
[39] U. Wittstadt, G. Füldner, O. Andersen, R. Herrmann, F. Schmidt, A new adsorbent composite material based on metal fiber technology and its application in adsorption heat exchangers, Energies 8 (8) (2015) 8431–8446.

[40] Y.I. Aristov, B. Dawoud, I.S. Glaznev, A. Elyas, A new methodology of studying the dynamics of water sorption/desorption under real operating conditions of adsorption heat pumps: experiment, Int. J. Heat Mass Transf. 51 (19–20) (2008) 4966–4972.
[41] McMaster-Carr - Weather- and Abrasion-Resistant Foam Strip, Blended EPDM with Adhesive-Back. [Online]. Available: https://www.mcmaster.com/#8694k111/=1ajm4w7. (accessed: 04-Dec-2017).
[42] F.P. Incropera, D.P. Dewitt, T.L. Bergman, A.S. Lavine, Fundam. Heat Mass Transfer. (2007).
[43] H. Czichos, T. Saito, L. Smith, Springer Handbook of Metrology and Testing, second ed., Springer, 2011.
[44] E. Tsotsas, H. Martin, Thermal conductivity of packed beds: a review, Chem. Eng. Process. 22 (1) (1987) 19–37.
[45] P. Teertstra, Thermal conductivity and contact Resistance measurments for adhesives, in: Proceedings of IPACK2007, 2007.
[46] M. Kaviany, Principles of Heat Transfer in Porous Media, Second Edi., 1995.
[47] VDI Heat Atlas, second ed. Springer, 2010.
[48] B. Dawoud, On the effect of grain size on the kinetics of water vapor adsorption and desorption into/from loose pellets of FAM-Z02 under a typical operating condition of adsorption heat pumps, J. Chem. Eng. Japan 40 (13) (2007) 1298–1306.
[49] J. P. Holman, Experimental Methods for Engineers, vol. 9, no. 2. 1994